Available online at www.sciencedirect.com
ScienceDirect
Journal of the European Ceramic Society 29 (2009) 2991–2998
www.elsevier.com/locate/jeurceramsoc

High temperature properties of ZnO ceramics studied by the impulse excitation technique

A.K. Swarnakar [a,*], L. Donzel [b], J. Vleugels [a], O. Van der Biest [a]

[a] *Department of Metallurgy and Materials Engineering, KULeuven, Kasteelpark Arenberg 44, B-3001 Leuven, Belgium*
[b] *ABB Switzerland, Corporate Research, Segelhofstrasse 1K, CH-5405 Dättwil, Switzerland*

Received 2 February 2009; received in revised form 22 April 2009; accepted 30 April 2009
Available online 29 May 2009

Abstract

This study reports on impulse excitation technique (IET) measurements up to 900 °C in air performed on various grades of ZnO ceramics, containing bismuth and antimony oxides as dopants. The IET provides dynamic elastic (E-modulus) and damping properties as a function of temperature. In order to correlate the IET behaviour with the microstructure and phase evolution, SEM and high temperature XRD (HT-XRD) analysis were carried out. Damping peaks related to phase transitions were observed in the samples containing Bi_2O_3 intergranular phase. Three other peaks are tentatively interpreted as point defect relaxations.

Keywords: Zinc oxide; Bismuth oxide; Antimony oxide; E-modulus; Damping; Impulse excitation technique

1. Introduction

Since the discovery of the varistor (variable-resistor) behaviour, zinc oxide (ZnO) ceramics have become important in electrical applications because of their highly non-linear electrical characteristics, which enable them to be used as reversible, solid-state switches with large-energy-handling capabilities for protection of electrical devices against overvoltages.[1]

Commercial varistors contain up to 10 different dopants, each added to optimize different aspects of the varistor performance.[1–4] Various studies have been done in order to understand the influence of the chemical composition on the electrical properties and grain growth behaviour of ZnO.[1,4–8] The special properties of the varistor are achieved during the sintering process, when the densification, phase formation, grain growth and doping take place. The most important dopant is bismuth oxide (Bi_2O_3), which is essential for the activation of the ZnO–ZnO grain boundaries, and promotes liquid phase sintering.[9] During cooling from the sintering temperature, the liquid Bi_2O_3 phase retracts to the triple points, leaving only a monolayer of Bi and O at the grain boundaries.[2,3,10–12] Antimony oxide (Sb_2O_3) is a dopant which inhibits grain growth of ZnO. It assists in binding the Bi_2O_3 by forming a pyrochlore phase and further reacts with ZnO to give a spinel phase.[13–15] Additionally, the presence of Bi may influence the lattice parameter of the spinel phase.[16,17]

IET is a well-recognized technique for the investigation of the high temperature behaviour of elastic modulus and internal friction or damping of various materials.[18–20] Information about processes taking place in the different phases of complex materials, such as a varistor ceramics, can be obtained by this technique.

In present work, IET studies were performed on ZnO ceramics with or without dopants. The elastic and damping behaviour of different ZnO material grades were investigated up to 900 °C in air. The microstructural investigation and XRD analysis were carried out before and after the IET measurement on each composition. High temperature X-ray diffractions (HT-XRD) were performed to study *in situ* phase transformation phenomena.

* Corresponding author. Tel.: +32 16 32 17 77; fax: +32 16 32 19 92.
E-mail addresses: akhileshkumar.Swarnakar@mtm.kuleuven.be (A.K. Swarnakar), lise.donzel@ch.abb.com (L. Donzel), jozef.vleugels@mtm.kuleuven.be (J. Vleugels), Omer.Vanderbiest@mtm.kuleuven.be (O. Van der Biest).

0955-2219/$ – see front matter © 2009 Elsevier Ltd. All rights reserved.
doi:10.1016/j.jeurceramsoc.2009.04.039

Table 1
Chemical compositions of the four studied materials.

Designation	Composition
ZN1	ZnO
ZN2	ZnO–2 mol% Bi_2O_3
ZN3	ZnO–2 mol% Bi_2O_3–3 mol% Sb_2O_3
ZNC	Commercial material (ZnO and Bi, Sb, Co, Mn, Ni)

2. Experimental details

2.1. Sample preparation

In addition to an Asian Commercial Varistor (ZNC), three different compositions were prepared, as listed in Table 1. High purity commercial ZnO, Bi_2O_3 and Sb_2O_3 powders were used (analysis grade, Merck). The samples were prepared by mixing and pressing the starting powders into green pellets. Compositions ZN1 and ZN3 were sintered at 1100 °C for 2 h and composition ZN2 was sintered at 900 °C for 2 h at a heating and cooling rate of 50 °C/h. A lower sintering temperature for the ZN2 grade was necessary in order to limit the ZnO grain growth and thus obtain samples with a sufficient toughness to allow IET measurements.

In order to study the high temperature elastic and damping properties by IET, samples were cut into rectangular shapes (40 mm × 6.5 mm × 4 mm approx.) with a diamond saw. The samples were then polished in order to remove possible surface cracks and reduce the risk of sample breaking during IET measurement.

For SEM/EDX analysis, samples were prepared through several steps of grinding and polishing. Initial grinding for each sample was performed with a 15 μm diamond abrasive solution for few minutes. After grinding, each sample was polished through a series of diamond abrasives ranging from 6 μm down to 1 μm; in the last step further polishing was done using colloidal silica.

2.2. Characterization methods

The surface microstructure was examined by scanning electron microscopy (SEM, XL30-FEG, FEI, Eindhoven, the Netherlands), equipped with an energy dispersive analysis system (EDS, EDAX, Tilburg, the Netherlands) for compositional analysis. X-ray diffraction (XRD, 3003-TT, Seifert, Ahrensburg, Germany) was carried out for phase identification, A *Johanna Otto HDK 2.4 X-ray furnace* was mounted for *in situ* high temperature diffraction measurements.

Fig. 1 shows a schematic diagram of the IET measurement system, including suspension of sample, excitation and signal capturing device. Inside the IET apparatus, the impulse of a light impact excites the suspended sample into the resonance frequency. The sample's vibration is collected through a tube by a microphone and the signal is processed by a software-based analysis program for the calculation of the resonance frequency and damping.[18]

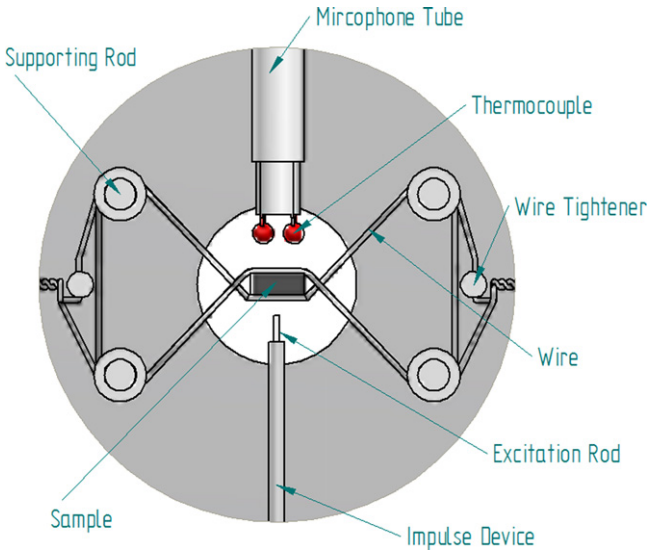

Fig. 1. A schematic diagram of the measurement set-up inside the IET furnace.

In the case of isotropic samples of rectangular shape, the elastic modulus of the materials can be calculated as[18]:

$$E = 0.9465\frac{m \cdot f_r^2}{b}\left(\frac{L}{t}\right)^3 \quad (1)$$

where E is the elastic modulus (Pa), f_r is the resonance frequency (Hz), m is the mass of the sample (g), and L, b and t are the length, width and thickness of the sample (mm), respectively.

The damping or internal friction (Q^{-1}) can be calculated from:

$$Q^{-1} = \frac{K}{\pi . f_r} \quad (2)$$

with K being the exponential decay parameter.

A furnace (*J.W. Lemmens*, Leuven, Belgium) was designed and equipped with automated impulse excitation and vibration detection devices, allowing computer-controlled measurements at temperatures up to 1100 °C in controlled environments. High temperature IET measurements were performed in air using Ni–Cr alloys thermocouple type-K wires to suspend the samples inside the furnace. A more detailed description of the equipment and the measuring technique can be found in published literature.[18–20]

3. Results

3.1. Microstructural analysis

The microstructure of a typical ZnO varistor consists of (i) ZnO grains, (ii) a Bi_2O_3 rich intergranular phase, (iii) spinel particles, mainly present in the triple junctions[13,21], and (iv) sometimes pyrochlore $Bi_3Sb_3Zn_2O_{14}$. The SEM micrographs on polished surfaces for the four different grades are shown in Fig. 2a–d. Due to the higher atomic weight of bismuth (Bi), the Bi_2O_3 phase appears as a white phase, whereas the spinel and ZnO appear light and dark grey respectively. The polished surfaces of the doped samples show a Bi-rich phase present at the

triple junctions. XRD analysis permits the identification of this phase as Bi_2O_3 in samples ZN2 and ZNC, and $Bi_3Sb_3Zn_2O_{14}$ pyrochlore in sample ZN3. In addition to the Bi-rich phases, the presence of zinc antimony and zinc cobalt antimony spinel grains was confirmed in grades ZN3 and ZNC, respectively. Due to the absence of sintering additives, ZN1 is rather porous as revealed by the black contrast in the SEM micrograph. The number of pores is drastically reduced in doped samples, as reported in Choi et al.[22] The grains of the commercial grade ZNC are much finer compared with ZN2 and ZN3. Full frame EDX analysis on ZNC indicates the presence of manganese (Mn), nickel (Ni) and cobalt (Co) beside Bi and Sb as doping elements (see Fig. 2d).

3.2. High temperature IET behaviour

The evolution of the E-modulus during heating, normalized with respect to the room temperature value, which are summarized in Table 2, is shown in Fig. 3. The four different ZnO ceramics were tested in air up to 900 °C with a heating and cooling rate of 2 °C/min. The E-modulus of pure ZnO (ZN1)

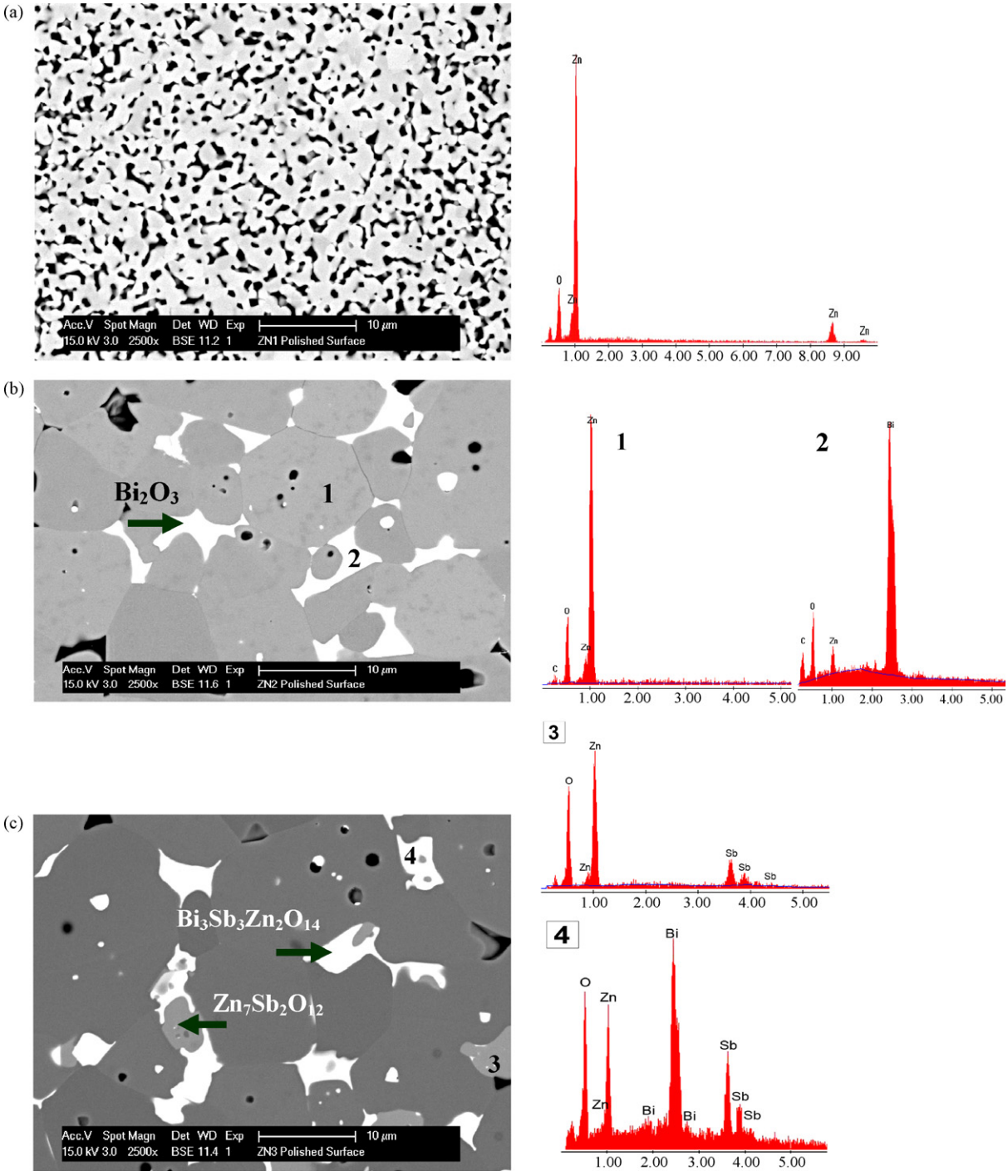

Fig. 2. High resolution SEM images of polished surfaces of grades ZN1 (a), ZN2 (b), ZN3 (c) and ZNC (d).

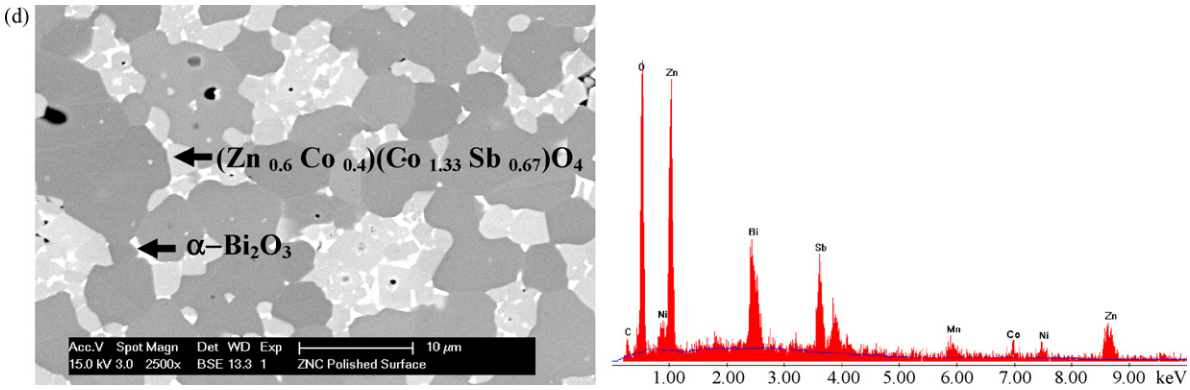

Fig. 2. (*Continued*).

slightly and steadily decreases with temperature. The ternary compound ZN3 (ZnO, Bi_2O_3 and Sb_2O_3) shows a decrease in the E-modulus similar to pure ZnO followed by a stronger decrease above 800 °C. The E-modulus of the ZNC (commercial) grade shows a small step at 400 °C, which is followed by a plateau between 500 and 600 °C, while the E-modulus strongly decreases above 650 °C. The binary compound ZN2 (ZnO and Bi_2O_3) exhibits an unexpected E-modulus behaviour, i.e., it decreases steeply up to 400 °C followed by a severe increase reaching a maximum at 650 °C. No reliable data were recorded by the system at temperatures above 670 °C.

The damping spectra of the four compositions are shown in Fig. 4a–d. The damping signals contain a lot of noise, however by considering measurements made on multiple samples the following features could be distinguished. For pure ZnO (ZN1), a damping peak (P_1) of very low amplitude, centred around 430 °C, and a small increase in the damping above 900 °C were observed. For the binary system (ZN2) two damping peaks located at 290 (P_2') and 450 °C (P_2'') respectively, can be distinguished and a steep increase in damping can be observed above 600 °C. The damping spectrum of the ternary system (ZN3) shows an exponential increase above 600 °C. The spectra of the commercial ZNC, shows a small peak (P_C') at 400 °C superimposed by a larger peak (P_C'') located around 500 °C before a further increase in damping takes place above 600 °C (Fig. 4d).

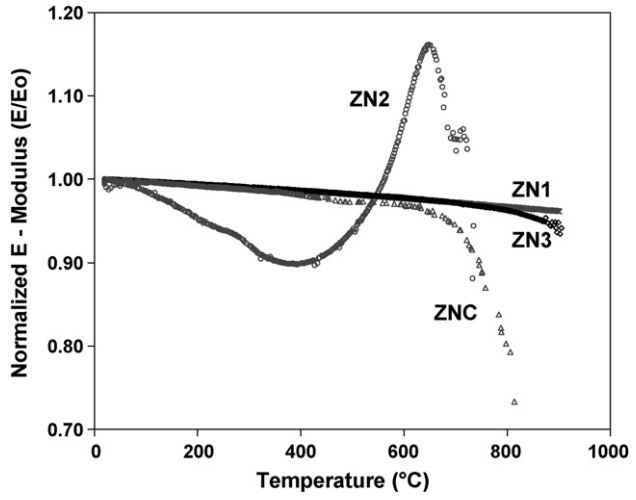

Fig. 3. Normalized E-modulus of different ZnO grades as a function of temperature.

3.3. X-ray diffraction analysis

XRD analysis was performed on pure and doped ZnO grades, before (at room temperature) and after the IET experiments (900 °C), as summarized in Fig. 5a. The results are summarized in Table 2, together with EDX analysis and E-modulus values. As expected, the diffraction pattern of pure ZnO sample (ZN1) contains only ZnO peaks before and after the IET measurement. In case of the binary system (ZN2), the initial $Bi_{38}ZnO_{58}$ phase transforms into γ-Bi_2O_3 after thermal cycling. Additionally, a weak reflection peak at $2\theta \approx 28.03°$ is attributed to tetragonal β-Bi_2O_3 (Fig. 5b). The three phases identified in the ternary system (ZN3), ZnO, $Bi_3Sb_3Zn_2O_{14}$ pyrochlore and $Zn_7Sb_2O_{12}$ orthorhombic spinel remained unchanged by the high temperature IET measurement. In the case of the commercial sample ZNC, zinc oxide $(Zn_{0.6}Co_{0.4})(Co_{1.33}Sb_{0.67})O_4$ spinel and α-Bi_2O_3 phases were detected before the IET measurement. After IET, γ-Bi_2O_3 phase was detected, due to the transformation of α-Bi_2O_3.

For each grade, the results of *in situ* high temperature X-ray diffraction measurements performed in air at temperatures from 300 to 650 °C are shown in Fig. 6. The highest intensity reflection peaks are those of ZnO. For each grade (Fig. 6a–d), a 2θ phase shift of the ZnO peak is observed within the measured temperature range. For example the 36.29° peak is observed at 36.18° at 600 °C. In the case of ZN2 (Fig. 6b), the $Bi_{38}ZnO_{58}$ phase was observed up to 400 °C while it transformed to γ-Bi_2O_3 at higher temperatures and remained stable up to 650 °C. The small β-Bi_2O_3 peak that was detected after the IET measurement up to 900 °C in Fig. 5b must originate from a partial transformation of γ-Bi_2O_3 at a temperature between 650 and 900 °C, which is beyond the measured HT-XRD range. ZN3 (Fig. 2c) shows that the ZnO, spinel and pyrochlore phases are stable over the whole measured temperature range. In case of ZNC (Fig. 2d), the ZnO and $(Zn_{0.6}Co_{0.4})(Co_{1.33}Sb_{0.67})O_4$ reflections are stable up to 650 °C. Other XRD peaks identified as α-Bi_2O_3 at room temperature transform into γ-Bi_2O_3 between 500 and 600 °C.

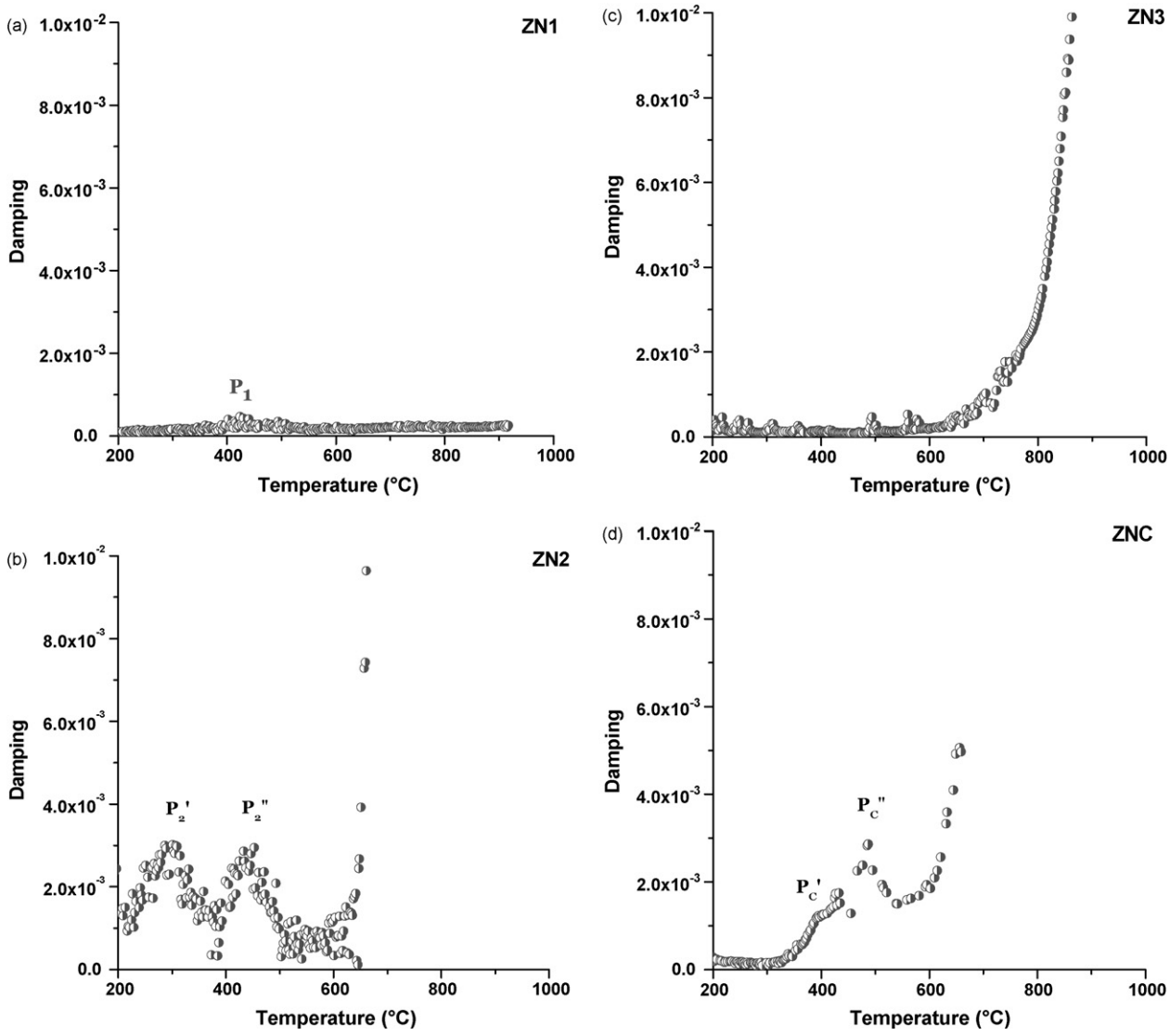

Fig. 4. Damping behaviour of ZnO samples as a function of temperature for ZN1 (a), ZN2 (b), ZN3 (c) and ZNC (d).

4. Discussions

Anelastic relaxation processes involving point defects, dislocations, grain boundaries or phase transitions are reflected in the mechanical spectra of a material. Point defects such as interstitials or vacancies can jump to the next site over an energy barrier E_b with a frequency:

$$\Gamma = \Gamma_0 \exp\left[-\frac{E_b}{k_b T}\right] \tag{3}$$

with the pre-exponential factor, Γ_0 being the lattice vibration frequencies, k_b the Boltzmann constant and T the absolute temperature.[23] An anelastic relaxation peak due to point defects can theoretically be described by the Debye equation:

$$\tan\phi = \Delta \frac{\omega\tau}{1+(\omega\tau)^2} \tag{4}$$

with $\omega = 2\pi f$ and $\tau = 1/\Gamma$ where Δ is the relaxation amplitude and f is the vibration frequency.

Different dissipation peaks are observed in the spectra of the ZnO samples. A single peak, P_1 in pure ZnO; two peaks, P_2' and P_2'', in the binary system; and two peaks P_C' and P_C'' in the commercial sample were deconvoluted. The spectra of the ternary sample do not contain dissipation peaks, up to 900 °C.

The P_2'' and P_C'' peaks in the binary and commercial material occur at the same temperature range at which phase transitions were observed in the HT-XRD. Moreover, the peaks are associated with an increase in the E-modulus (see Fig. 3). In the binary system, the $Bi_{38}ZnO_{58}$ phase changes to γ-Bi_2O_3 between 400 and 450 °C. The crystal structure of $Bi_{38}ZnO_{58}$ is analogous to the bcc based γ-Bi_2O_3 solid solution, but differs by the slight increase of the lattice parameter from 1.0206 to 1.0267 (nm). The increase of the E-modulus from 400 °C can be associated with the volume expansion due to $Bi_{38}ZnO_{58}$ to γ-Bi_2O_3 transition. Currently, it is not clear why the E-modulus drops between room temperature and 400 °C during heating. Further research is required for more explanation about this unexpected behaviour. In the commercial ZNC sample, the α-Bi_2O_3 phase changes to

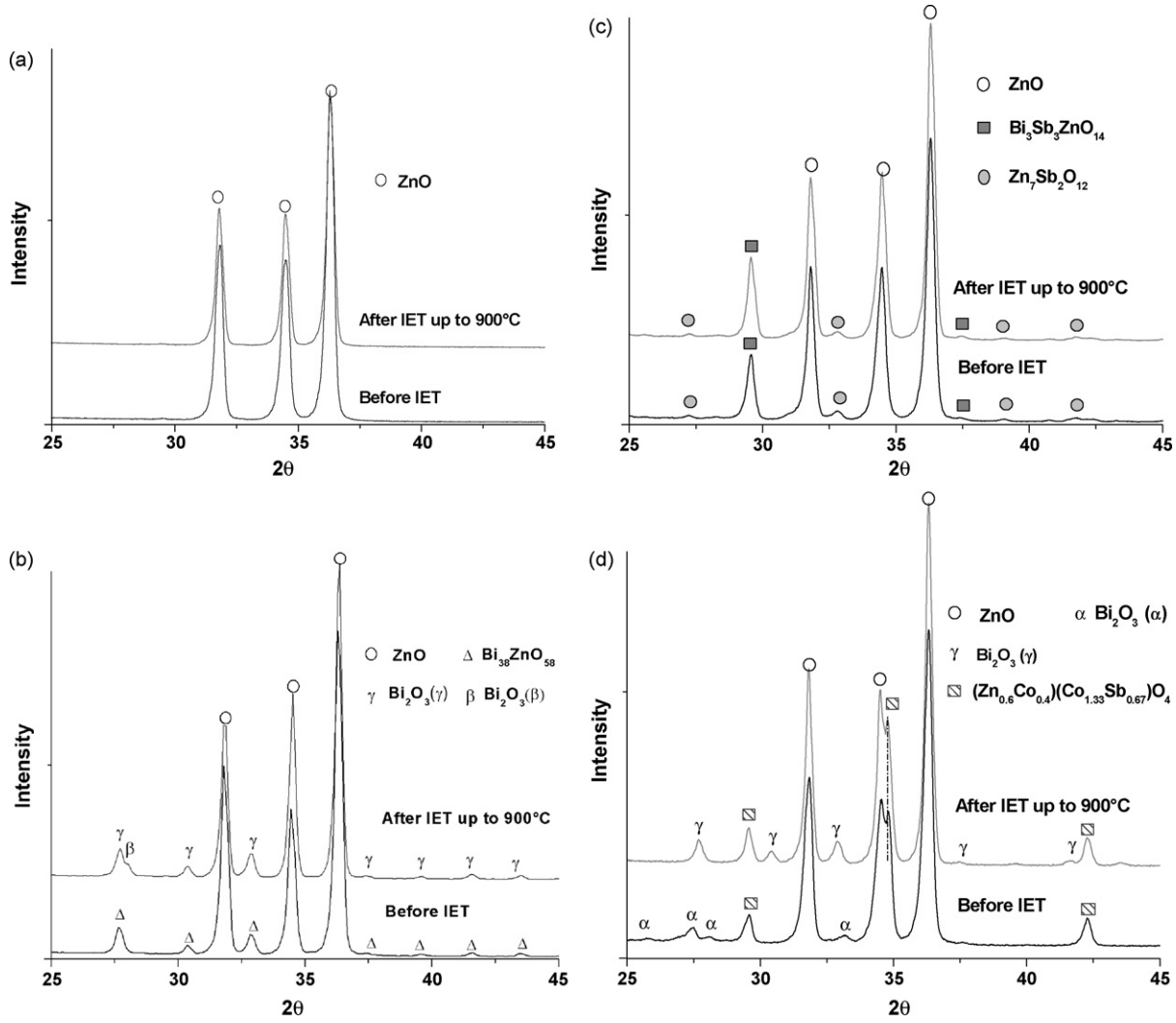

Fig. 5. XRD pattern of the ZN1 (a), ZN2 (b), ZN3 (c) and ZNC (d) before and after IET testing up to 900 °C.

γ-Bi_2O_3 between 500 and 550 °C. The cubic γ-phase has a larger unit cell than the monoclinic α-phase. So for both materials, the stiffening of the material can be explained by the volume expansion of the intergranular Bi-phase and the damping peak related to atomic motion associated with the phase transition. The effect is stronger in the ZN2 sample that contains more intergranular Bi phase as can be seen in the SEM observations (Fig. 2b).

For the other peaks, there is no indication from the XRD analysis that they might be related to phase changes. Unfortunately, we could not change the geometry of the sample to achieve resonance frequencies significantly different to determine if these peaks are thermally activated and if so to assess the activation energy. Assuming that these peaks are Debye peaks and that the lattice vibration frequency is 10^{13} s[23,24], the ampli-

Table 2
Summary of the results for all ZnO grades.

	ZnO grade			
	ZN1	ZN2	ZN3	ZNC
E-modulus (±3) GPa	96	73	109	112
EDX analysis	Zn, O	Zn, O, Bi	Zn, O, Bi, Sb	Zn, O, Bi, Sb, Co, Ni, Mn
XRD analysis (before IET experiments)	ZnO	ZnO, $Bi_{38}ZnO_{58}$	ZnO, $Zn_7Sb_2O_{12}$, $Bi_3Sb_3Zn_2O_{14}$	ZnO, α-Bi_2O_3, $(Zn_{0.6}Co_{0.4})(Co_{1.33}Sb_{0.67})O_4$
XRD analysis (after IET experiments)	ZnO	ZnO, γ-Bi_2O_3, traces of β-Bi_2O_3	ZnO, $Zn_7Sb_2O_{12}$, $Bi_3Sb_3Zn_2O_{14}$	ZnO, γ-Bi_2O_3, $(Zn_{0.6}Co_{0.4})(Co_{1.33}Sb_{0.67})O_4$
$(d(E/E_0))/dT$ (K^{-1}) (RT to 250 °C)	-4×10^{-5}	-2×10^{-4}	-4×10^{-5}	-4×10^{-5}

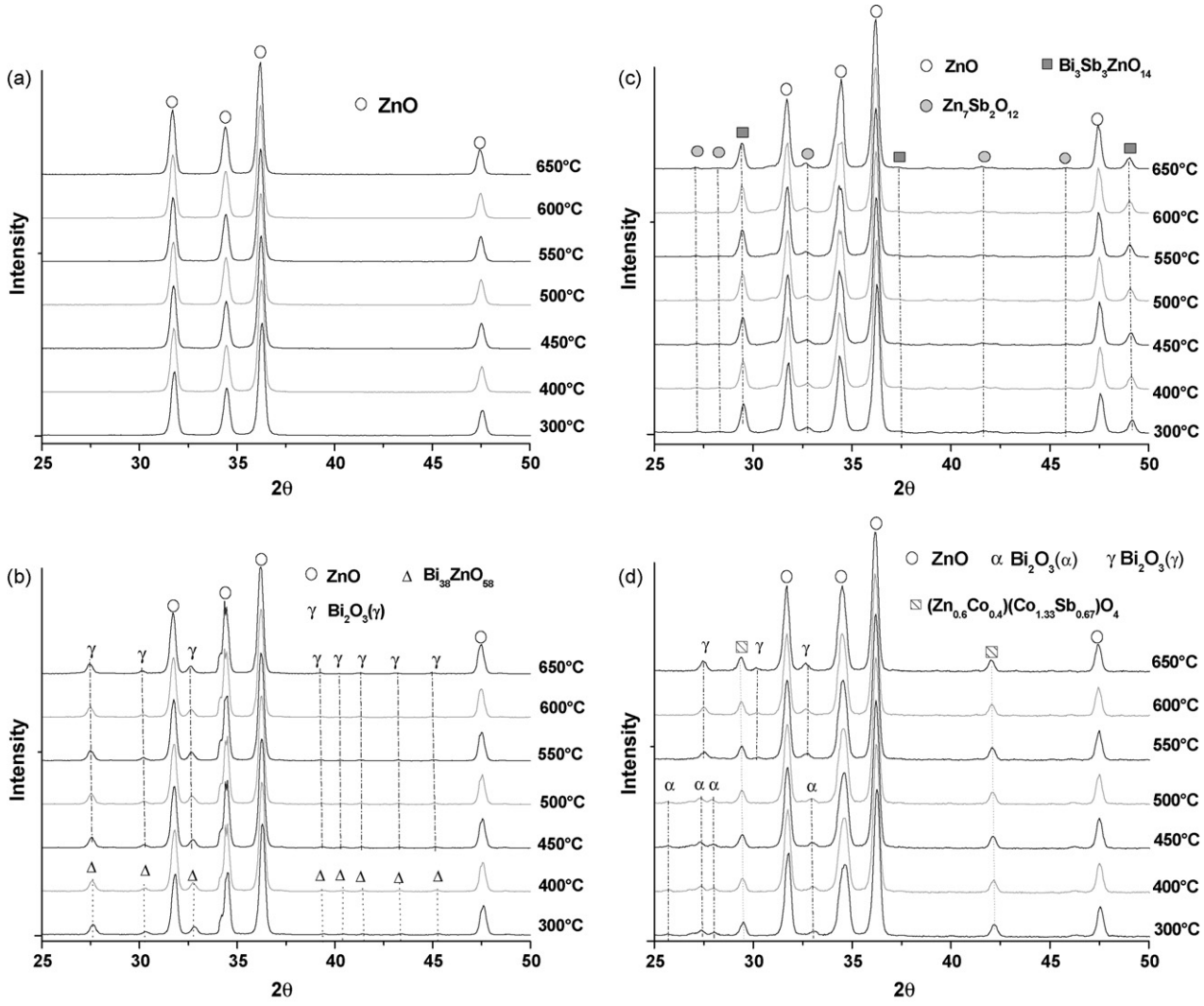

Fig. 6. High temperature X-ray diffraction from 300 to 650 °C for ZN1 (a), ZN2 (b), ZN3 (c) and ZNC (d) grades.

tude and activation energy were determined and summarized in Table 3.

As possible interpretation of the low intensity-damping peak P_1, we propose that the peak could correspond to the point defects inside the ZnO crystal. However, the nature of the point defect is not clear. Diffusion experiments have shown that the activation energies for Zn and O, 3.3 and 3.96 eV respectively[25], are much higher than the 1.14 eV estimated here. The values are believed to be so large because they involve the point defect formation energy as well. So, if P_1 is indeed due to point defects, one possible explanation for the smaller value determined in the present study is that some involuntary doping of the ZN1 sample occurred during sintering due to contamination in the oven thus generating some extrinsic point defects.

Table 3
Amplitude and activation energy assuming that the peaks are Debye peaks, assuming an attempt frequency of 10^{13} s[24].

Peak	Peak temperature (°C)	Peak frequency (kHz)	Δ	E (eV)
P_1 (ZN1)	430	11.15	0.3×10^{-3}	1.14
P_2' (ZN2)	290	13.8	4.5×10^{-3}	0.91
P_C' (ZNC)	400	13.9	1.8×10^{-3}	1.08

The damping peaks (P_2' and P_2'') in the binary system (ZN2) must originate from the Bi-phase, as similar peaks are not observed in the pure ZnO sample. As already mentioned above the P_2'' can be correlated to the phase transition of the intergranular Bi-phase from $Bi_{38}ZnO_{58}$ to γ-Bi_2O_3. We propose that the P_2' peak and the associated drop of the elastic modulus could be due to point defects in the Bi-phase. Russwurm[26] reported that the activation energy of the ionic conductivity of γ-Bi_2O_3 is 0.99 V which is close to the estimated activation energy value for peak P_2' (Table 3).

The ternary system (ZN3) consists of ZnO, $Bi_3Sb_3Zn_2O_{14}$ pyrochlore and $Zn_7Sb_2O_{12}$ spinel. These phases are stable up to at least 650 °C (maximum temperature of the HT-XRD measurements). We propose that the sharp drop in E-modulus and the exponential increase of the damping might be due to the decomposition of $Bi_3Sb_3Zn_2O_{14}$ into spinel and liquid Bi_2O_3, which can occur at 850 °C as reported by Metz et al.[27] For ZNC, as mentioned above P_C'' can be associated with the α to γ phase

change. Limited knowledge of the material composition makes it difficult to identify the origin of P_C'. EDX analysis (full frame) has shown the presence of some doping elements such as Co, Mn, Ni etc., which may play a role in the damping peak P_C' and the associated minor E-modulus drop, observed at around 400 °C. Possibly, the major softening and the exponential damping background observed above 650 °C could be related to the softening and melting of the Bi_2O_3 intergranular phase.

5. Conclusions

Four grades of ZnO were studied for their elastic and damping properties as a function of temperature by using IET. In pure ZnO (ZN1), the E-modulus decreases linearly with temperature by 5% up to 900 °C and a small damping peak, presumably due to extrinsic point defects, was observed at 450 °C. The binary ZnO–Bi_2O_3 system (ZN2) shows an intergranular Bi-phase. The origin of the damping peak P_2' seen at 290 °C in that material is tentatively attributed to point defect relaxation in the Bi_2O_3 phase. The increase of the E-modulus and associated damping peak at P_2'' are related to the transition from $Bi_{38}ZnO_{58}$ to γ-Bi_2O_3 that was confirmed by HT-XRD. The ternary ZnO–Bi_2O_3–Sb_2O_3 system (ZN3) has a continuous decrease in E-modulus, which is similar to pure ZnO up to the 800 °C. The sharp decrease in modulus above 850 °C could be due to the decomposition of the $Bi_3Sb_3Zn_2O_{14}$ pyrochlore phase. In the commercial material (ZNC), the HT-XRD observation allows us to attribute the anomaly in the $E/E_0(T)$ curve and the damping peak P_C'' at around 500 °C to the α to γ-Bi_2O_3 phase transition. The additional peak at 400 °C (P_C') could be related to the presence of doping elements in the commercial material. The modulus drop and exponential increase of the damping observed above 650 °C might be due to the melting of the Bi_2O_3 intergranular phase.

Acknowledgements

This work was performed within the framework of the Research Fund of K.U. Leuven under project GOA/08/007and FWO project grant number 3E060133. The authors are grateful to R. Kessler and F. Greuter for fruitful discussion.

References

1. Matsuoka, M., Nonohmic properties of zinc oxide ceramics. *Jpn. J. Appl. Phys.*, 1971, **6**, 736–746.
2. Peiteado, M., de la Rubia, M. A., Velasco, M. J., Valle, F. J. and Caballero, A. C., Bi_2O_3 vaporization from ZnO-based varistors. *J. Eur. Ceram. Soc.*, 2005, **9**, 1675–1680.
3. Levinson, L. M., Advances in varistor technology. *Ceram. Trans.*, 1989.
4. Clarke, D. R., Varistor ceramics. *J. Am. Ceram. Soc.*, 1999, **3**, 485–502.
5. Özgür, Ü., Alivov, Ya. I., Liu, C., Teke, A., Reshchikov, M. A., Dogan, S., Avrutin, V., Cho, S. J. and Morkoçd, H., A comprehensive review of ZnO materials and devices. *J. Appl. Phys.*, 2005, 041301.
6. Senda, T. and Bradt, R. C., Grain growth of zinc oxide during the sintering of zinc oxide-antimony oxide ceramics. *J. Am. Ceram. Soc.*, 1991, **6**, 1296–1302.
7. Levinson, L. M. and Philipp, H. R., Zinc oxide varistors—a review. *J. Am. Ceram. Soc.*, 1986, **4**, 639–646.
8. Greuter, F. and Blatter, G., Electrical properties of grain boundaries in polycrystalline compound semiconductors. *Semicond. Sci. Technol.*, 1990, 111–137.
9. Greuter, F., Electrically active interfaces in ZnO varistors. *Solid State Ionics Interf. Ionic Mater.*, 1995, 67–78.
10. Greuter, F. and Stucki, F., Key role of oxygen at zinc oxide varistor grain boundaries. *Appl. Phys. Lett.*, 1990, 446–449.
11. Clarke, D. R., The microstructural location of the intergranular metal-oxide phase in a zinc oxide varistor. *J. Appl. Phys.*, 1978, 2407–2411.
12. Lee, J. R., Chiang, Y. M. and Ceder, G., Pressure-thermodynamic study of grain boundaries: Bi segregation in ZnO. *Acta Mater.*, 1997, **45**(3), 1247–1257.
13. Balzer, B., Hagemeister, H., Kocher, P. and Gauckler, L. J., Mechanical strength and microstructure of zinc oxide varistor ceramics. *J. Am. Ceram. Soc.*, 2004, **10**, 1932–1938.
14. Kim, J., Kimura, T. and Yamaguchi, T., Sintering of zinc oxide doped with antimony oxide and bismuth oxide. *J. Am. Ceram. Soc.*, 1989, **8**, 1390–1395.
15. Inada, M., Formation mechanism of nonohmic zinc oxide ceramics. *Jpn. J. Appl. Phys.*, 1980, 409–419.
16. Vasantha Kumari, K. G., Divya Vasu, P., Kumar, V. and Asokan, T., Formation of zinc–antimony-based spinel phases. *J. Am. Ceram. Soc.*, 2002, **3**, 703–705.
17. Haskell, B. A., Souri, S., Helfand, J. and Varistor, M. A., Behavior at twin boundaries in ZnO. *J. Am. Ceram. Soc.*, 1999, **8**, 2106–2110.
18. Roebben, G., Bollen, B., Brebels, A., Van Humbeeck, J. and Van Der Biest, O., Impulse excitation apparatus to measure resonant frequencies, elastic moduli, and internal friction at room and high temperature. *Rev. Sci. Instrum.*, 1997, **12**, 4511–4515.
19. Gimenez, S., Lauwagie, T., Roebben, G., Heylen, W. and Van der Biest, O., Effects of microstructural heterogeneity on the mechanical properties of pressed soft magnetic composite bodies. *J. Alloys Compd.*, 2006, **1–2**, 299–305.
20. ASTM E 1876-99, *ASTM Committee E-28 on Mechanical Testing, Subcommittee E2803 on Elastic Properties*, 2000.
21. Olsson, E. and Dunlop, G. L., The effect of Bi_2O_3 content on the microstructure and electrical properties of ZnO varistor materials. *J. Appl. Phys.*, 1989, **9**, 4317–4324.
22. Choi, J. H., Hwang, N. M. and Kim, D. Y., Pore–boundary separation behavior during sintering of pure and Bi2O3-doped ZnO ceramics. *J. Am. Ceram. Soc.*, 2001, **6**, 1398–1400.
23. Nowick, A. S. and Berry, B. S., *Anelastic Relaxation in Crystalline Solid*. Academic Press, New York, London, 1972.
24. Janotti, A. and Van de Walle, C. G., Native point defects in ZnO. *Phys. Rev. B: Conden. Matter Mater. Phys.*, 2007, **16**, 165202–165222.
25. Kaldis, E. and Sirtl, E., Current topics in materials science. *J. Electrochem. Soc.*, 1980, **7**, 283C–284C.
26. Russwurm, W., *Strukturelle und elektrische Eigenschaften von ZnO-Varistorkeramik und deren Bi_2O_3-haltigen Nebenphasen*. PhD Thesis, Universitat Regensburg, 1987.
27. Metz, R., Delalu, H., Vignalou, J. R., Achard, N. and Elkhatib, M., Electrical properties of varistors in relation to their true bismuth composition after sintering. *Mater. Chem. Phys.*, 2000, **2**, 157–162.